



Construction and Validation of a risk model Based on Cuprotosis-related LncRNAs in Colon Adenocarcinoma

Pufang Tan¹, Renshan Hao¹, Qi Zhu^{1,2}, Xiao Wu³, Ye Zhang^{4*}

¹Division of Gastroenterology and Hepatology, Baoshan Branch, Ren Ji Hospital, Shanghai Jiao Tong University School of Medicine, Shanghai, 200444, China

²Division of Gastroenterology and Hepatology, Key Laboratory of Gastroenterology and Hepatology, Ministry of Health, Ren Ji Hospital, Shanghai Jiao Tong University School of Medicine; Shanghai Institute of Digestive Disease, Shanghai, 200127, China

³Oncology Department, The First Affiliated Hospital of Bengbu Medical College, Bengbu, 233000, China

⁴Laboratory of Medicine, Baoshan Branch, Ren Ji Hospital, Shanghai Jiao Tong University School of Medicine, Shanghai, 200444, China

ARTICLE INFO

Original paper

Article history:

Received: June 20, 2022

Accepted: November 20, 2022

Published: December 31, 2022

Keywords:

Cuprotosis, Colon adenocarcinoma, Long noncoding RNA, Prognosis

ABSTRACT

Cancer cells are significantly impacted by copper-induced cell death (cuprotosis). Long noncoding RNAs (lncRNAs) are crucial in the developmental process of colon adenocarcinoma (COAD). The ability of Cuprotosis-related lncRNA biomarkers to predict COAD prognosis, on the other hand, remains uncertain. This research intended to build a model of risk specifically for COAD based on cuprotosis-related lncRNAs. Univariable Cox, LASSO, as well as multivariable Cox analyses were utilized to identify cuprotosis-related lncRNAs linked with prognosis, and a model of risk was constructed. Five cuprotosis-related lncRNAs, AC008494.3, SNHG7, LINC02257, ZEB1-AS1, and AC116913.1, were discovered from the training set and utilized for the creation of a predictive model of risk. In the training and testing sets, as well as the total patient population, overall survival was dramatically lower for the high-risk patients than for the low-risk patients. The model's prognosis validity was confirmed by time-dependent areas under the ROC curves, which were identified as an independent prognosis element in multivariable COX regressive analysis. The established cuprotosis-related lncRNA-based predictive risk model was linked to chemotherapeutic sensitivity. In COAD patients, a model of risk based on five cuprotosis-related lncRNAs can predict prognosis and chemotherapeutic effectiveness.

Doi: <http://dx.doi.org/10.14715/cmb/2022.68.12.16>

Copyright: © 2022 by the C.M.B. Association. All rights reserved.

Introduction

Colon adenocarcinoma (COAD) is the second most lethal and the third most prevalent malignancy tumor (1-3). Despite advances in treatment and early diagnosis, the 5-year survivorship rate is still just 50% (4-6). The TNM staging system is an excellent instrument for evaluating the disease severity, determining the therapy strategy, evaluating the treatment efficacy, and predicting prognosis in patients with COAD (7). However, some patients of the same TNM stage have different prognoses (8, 9). Therefore, innovative molecular biomarkers for forecasting the prognosis and therapeutic efficacy of COAD sufferers are urgently required.

Copper is a trace element that is maintained at extremely low amounts in cells through a homeostatic mechanism. Once the threshold is exceeded, copper becomes poisonous and causes the death of cells through cuprotosis, a separate type of cell death (i.e., apoptosis, pyroptosis, necrosis, and ferroptosis). Cuprotosis may cause fatty acylated proteins to aggregate and subsequent downregulation of iron-sulfur clustering proteins, ultimately leading to proteotoxic stress and cell death (10). Studies (11) have shown that copper promotes colon tumor growth by promoting mutations in KRAS and that blocking macropinocytosis can block copper uptake, copper-dependent signaling, and tumor growth. Long noncoding RNAs (lncRNAs) are noncod-

ing RNAs whose length exceeds 200 nucleotides (12, 13), which is pivotal for the onset and developmental process of colon cancer (14-16). However, a cuprotosis-related lncRNA model to forecast COAD sufferers' prognosis has not been reported. This work aimed to develop a marker model of risk for forecasting the prognoses of COAD sufferers according to lncRNAs associated with cuprotosis.

Materials and Methods

Data collecting

RNA expression datasets and clinical features from COAD sufferers were obtained from TCGA on the website of <https://portal.gdc.cancer.gov/>, including 473 COAD tissues and 41 paracancerous normal tissue samples. On the website of <https://portal.gdc.cancer.gov/>, TCGA datasets and clinical information from COAD sufferers were harvested, including 473 COAD tissues and 41 paracancerous normal tissue samples. Nineteen genes related to cuprotosis were collected from relevant literature (10, 11, 17-20). In order to distinguish cuprotosis-related lncRNAs, a coexpression analysis of cuprotosis-related genes and lncRNAs was conducted. We adopted Pearson's correlative analysis to compute correlative coefficients between cuprotosis-associated genes and lncRNAs, and correlative coefficients > 0.4 with $P < 0.001$ were deemed significant.

Identification and validation of lncRNA risk biomar-

* Corresponding author. Email: mosi07755141077@163.com

kers associated with cuprotosis

COAD sufferers were stochastically separated into training or testing sets for the purpose of identifying and validating lncRNA risk biomarkers. In the training set, univariable Cox analyses were utilized to determine cuprotosis-associated lncRNAs linked to overall survival (OS), which were subsequently analyzed with LASSO. The identified cuprotosis-related lncRNAs were then incorporated into a multivariable Cox analysis to develop a model of risk. The risk score of every COAD sufferer was obtained via the formula below: risk score = $\sum \beta_i S_i$, where β_i as the regression coefficient, and S_i as the lncRNA expression value. Based on the median risk score, COAD sufferers were separated into high- and low-risk groups. To study the predictive influence of the risk score on the clinical prognosis of COAD sufferers, survivorship curves were produced via K-M Plotter to compare survivorship between these groups. We used ROC curves to estimate predictive performance and used the area under the ROC curve (AUC) to quantify predictive power.

It was determined using univariable and multivariable Cox analyses if the risk scoring was an independent prognosis element for COAD sufferers. Additionally, a multi-index ROC curve was established to analyze the risk score's ability to forecast risk.

Development and validation of a nomograph

We built a nomograph as a quantitative predictor of clinical prognoses using the "rms" R package by merging five cuprotosis-related lncRNAs with clinicopathological features. The accuracy of the forecast was evaluated via a correction chart, which illustrated the variance between forecasted and real survivorship, with the 45-degree line being the ideal forecast outcome.

Chemotherapeutic medication sensitivity evaluation

We utilized the pRRophetic R package for calculating the 50% maximum inhibitory concentration (IC50) of commonly used chemo medicines in order to assess the prognosis model's predictive effect on the basis of cuprotosis-related lncRNAs on drug treatment effects in patients with COAD. Comparing the IC50 values between the two risk groups was completed via the Wilcoxon test; $P < 0.001$ had significance on statistics.

Statistical analysis

Using the Chi-square test, the clinical and pathological features of high-risk and low-risk sufferers were compared. The survivorship curve approach was employed to compare the OS between the two groups, and the log-rank test was utilized to identify the diversity in OS. For statistical analysis, the R software package was employed, and $P < 0.05$ had significance on statistics.

Results

Basic clinicopathological information about the study's COAD patients

This study included 446 COAD patients (Table 1), who were evenly allocated at random to either the training or testing set ($n = 223$, each). In the training and testing sets, the clinicopathological characteristics (age, sex, TNM stage, etc.) were not statistically different ($P > 0.05$).

Screening of cuprotosis-related lncRNAs linked with prognosis in training set

We used 19 938 mRNAs and 16 876 lncRNAs in the TCGA database to generate an expression matrix, and 19 genes related to cuprotosis were identified with reference to relevant literature (10, 11, 17-20). Pearson correlation

Table 1. Clinicopathological features of COAD research participants.

Clinical variables		Total (n = 446)	Training set (n = 223)	Testing set (n = 223)	P value
Age	≤65	183 (41.03%)	100 (44.84%)	83 (37.22%)	0.1235
	>65	263 (58.97%)	123 (55.16%)	140 (62.78%)	
Sex	Female	212 (47.53%)	107 (47.98%)	105 (47.09%)	0.9245
	Male	234 (52.47%)	116 (52.02%)	118 (52.91%)	
Stage	I	75 (16.82%)	41 (18.39%)	34 (15.25%)	0.4521
	II	175 (39.24%)	79 (35.43%)	96 (43.05%)	
	III	124 (27.8%)	65 (29.15%)	59 (26.46%)	
	IV	61 (13.68%)	29 (13%)	32 (14.35%)	
	Unknown	11 (2.47%)	9 (4.04%)	2 (0.9%)	
T Stage	T1	10 (2.24%)	7 (3.14%)	3 (1.35%)	0.4045
	T2	76 (17.04%)	40 (17.94%)	36 (16.14%)	
	T3	303 (67.94%)	145 (65.02%)	158 (70.85%)	
	T4	56 (12.56%)	31 (13.9%)	25 (11.21%)	
	Tis	1 (0.22%)	0 (0%)	1 (0.45%)	
M Stage	M0	329 (73.77%)	164 (73.54%)	165 (73.99%)	0.8481
	M1	61 (13.68%)	29 (13%)	32 (14.35%)	
	unknown	56 (12.56%)	30 (13.45%)	26 (11.66%)	
N Stage	N0	265 (59.42%)	131 (58.74%)	134 (60.09%)	0.6133
	N1	102 (22.87%)	55 (24.66%)	47 (21.08%)	
	N2	79 (17.71%)	37 (16.59%)	42 (18.83%)	

COAD: colon adenocarcinoma.

analysis revealed 1724 lncRNAs linked with cuprotosis. 48 cuprotosis-related lncRNAs with prognosis significance in COAD sufferers were found using univariable Cox analysis (Table S1).

Identification of cuprotosis-related lncRNAs risk biomarkers in the training set

The 48 cuprotosis-related lncRNAs in the training set were analyzed using LASSO regression, and 10 cuprotosis-related lncRNAs linked with prognosis were identified (AC022210.1, CCDC28A-AS1, RPARP-AS1, AC008494.3, SNHG7, LINC02257, ZEB1-AS1, AP001160.1, and AC116913.1) (Figure 1). Multivariable Cox analysis was conducted on these 10 lncRNAs, and five lncRNAs linked with cuprotosis and the prognosis of COAD patients (AC008494.3, SNHG7, LINC02257, ZEB1-AS1, and AC116913.1) were used to establish a prediction model. The coefficients and hazard ratios (HR) of the significant lncRNAs are shown in Table 2. The mid-value of risk scores was utilized to distribute training set sufferers into high- and low-risk groups. Figures 2A and B illustrate the distributional status of risk score and the probability of survivorship. Among high-risk populations, there were more fatalities and survivorship time was shorter. Five significant prognostic lncRNAs' expression features were visualized using a heatmap (Figure 2C). Four risk-type lncRNAs, SNHG7, LINC02257, ZEB1-AS1, and AC116913.1, had increased expression levels in the high-risk individuals. AC008494.3, a protective lncRNA, was expressed at a lower level in the high-risk populations. Sufferers at low risk had significantly higher survivorship (Figure 2D). Using ROC curve analysis, the accurateness of a prognostic model on the basis of cuprotosis-related lncRNA biomarkers was evaluated. AUC = 0.845 for the 5-year survivorship rate in the training set was greater than AUC = 0.753 for the 3-year survivorship rate and AUC = 0.743 for the 1-year survivorship rate (Figure 2E).

Validation of the cuprotosis-related lncRNA model of risk in the testing set and total patient population

We also generated risk scores for the testing set and total patient population and split the patients into two risk groups. Sufferers at high risk had a shorter average survivorship time and more fatalities (Figure 3A-D). A heatmap of the expression profiles of five significantly prognostic lncRNAs (SNHG7, LINC02257, ZEB1-AS1, and AC116913.1) revealed that the levels of risk-type lincR-

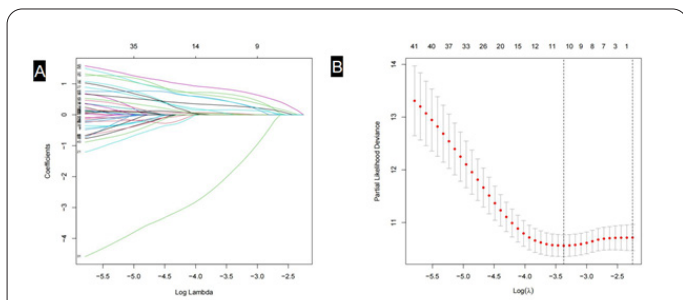


Figure 1. Filtering graph of lncRNAs associated with survival in patients with COAD. (A) In the LASSO coefficient spectrum of 48 prognostic cuprotosis-related lncRNAs in COAD, a coefficient distribution map is constructed for a logarithmic sequence. (B) In the LASSO model, the COAD optimum parameters are determined.

NAs were markedly elevated in high-risk sufferers. The level of the protective-type lncRNA AC008494.3 was lower in sufferers at high risk (Figures 3E and F). The survivorship rate of low-risk sufferers was much greater of high-risk sufferers (Figure 3G and H). The AUC of the testing set was 0.526, 0.623, and 0.663 at 5, 3, and 1 years, respec-

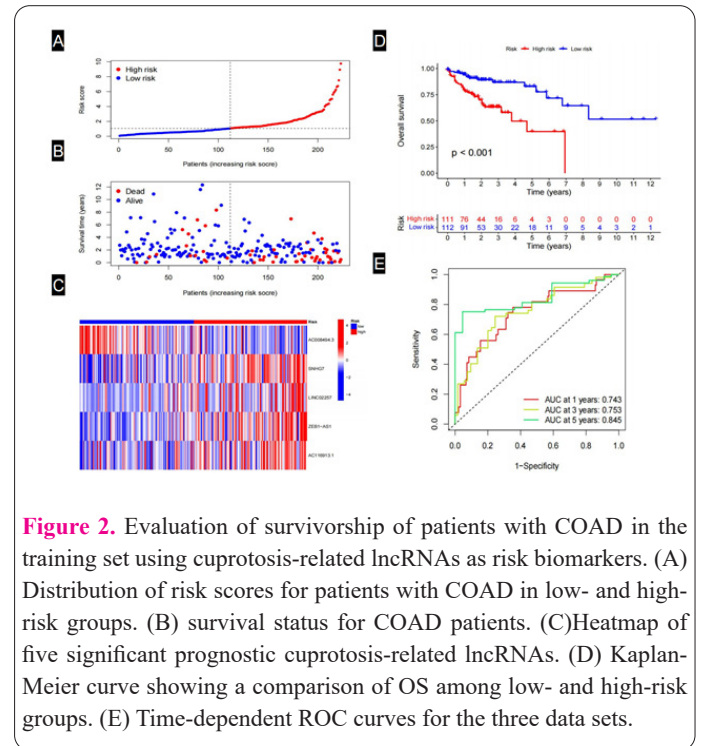


Figure 2. Evaluation of survivorship of patients with COAD in the training set using cuprotosis-related lncRNAs as risk biomarkers. (A) Distribution of risk scores for patients with COAD in low- and high-risk groups. (B) survival status for COAD patients. (C) Heatmap of five significant prognostic cuprotosis-related lncRNAs. (D) Kaplan-Meier curve showing a comparison of OS among low- and high-risk groups. (E) Time-dependent ROC curves for the three data sets.

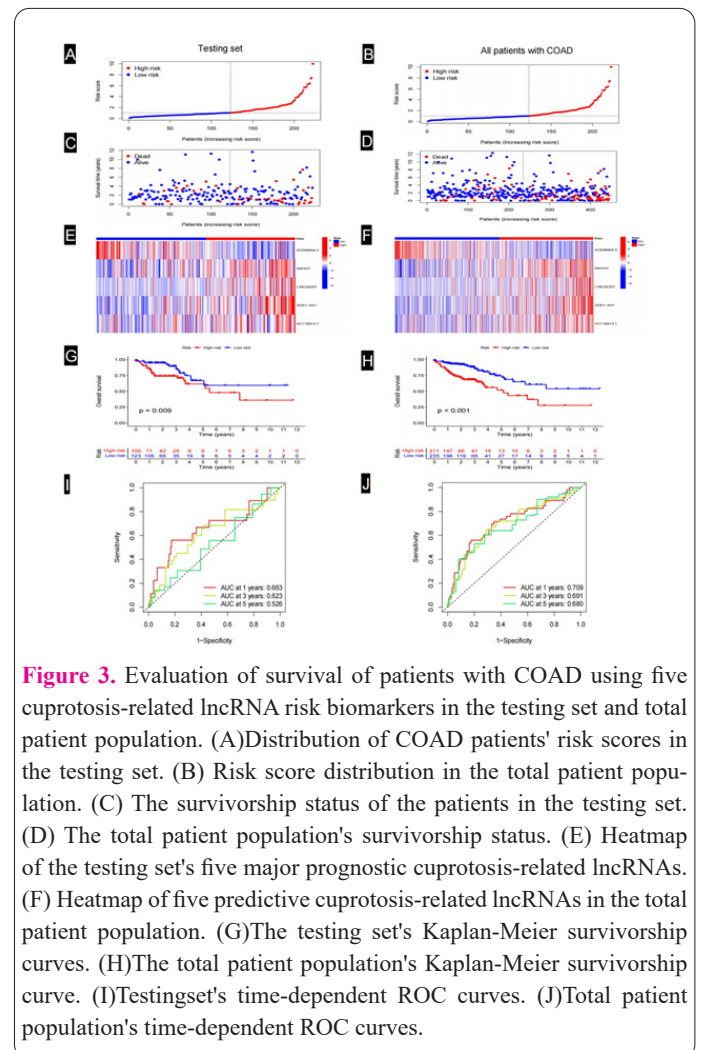


Figure 3. Evaluation of survival of patients with COAD using five cuprotosis-related lncRNA risk biomarkers in the testing set and total patient population. (A) Distribution of COAD patients' risk scores in the testing set. (B) Risk score distribution in the total patient population. (C) The survivorship status of the patients in the testing set. (D) The total patient population's survivorship status. (E) Heatmap of the testing set's five major prognostic cuprotosis-related lncRNAs. (F) Heatmap of five predictive cuprotosis-related lncRNAs in the total patient population. (G) The testing set's Kaplan-Meier survivorship curves. (H) The total patient population's Kaplan-Meier survivorship curve. (I) Testing set's time-dependent ROC curves. (J) Total patient population's time-dependent ROC curves.

tively (Figure 3I). The AUC for the entire patient population was 0.680, 0.691, and 0.709 at 5, 3, and 1 years, respectively (Figure 3J). Throughout these three time points, the prediction performance exhibited a gradually increasing trend. Analysis of the ROC curve demonstrated that the cuprotosis-related lncRNA marker-based prognostic model had a good predictive performance.

Correlation analysis of cuprotosis-related lncRNA risk biomarkers and clinicopathological features with OS in COAD patients

Univariable and multivariable Cox analyses unveiled that risk score, stage, and age can be adopted as prognostic indicators (Figures 4A and B). Risk biomarkers based on five cuprotosis-related lncRNAs are independent prognostic factors. The AUC of the risk score was 0.709, which was considerably higher than the AUCs of age (0.621), sex (0.480), and stage (0.705) (Figure 4C). The results showed that a risk model including these five lncRNAs had a good predictive performance for patient survival.

Development and validation of a nomograph

We developed a nomograph to predict OS at the first, third, and fifth year on the basis of the five cuprotosis-related lncRNAs and clinicopathological characteristics. As illustrated in Figure 5A, the score for each variable in the nomograph can be found in the score table, and the overall score was used to predict the 1-, 3-, and 5-year survivorship possibility. The nomograph was analyzed via a correction curve. The results demonstrated that the projected curve was near the ideal curve, and the prediction performance of the nomograph was favorable (Figure 5B).

Prediction of chemotherapeutic efficacy based on cuprotosis-related lncRNA biomarkers

The IC50 levels of the chemotherapeutic drugs elesclomol, NU-7441, PI-103, AUY922, CEP-701, OSI-027, axitinib, cisplatin, KU-55933, PF-4708671, TW37, camp-

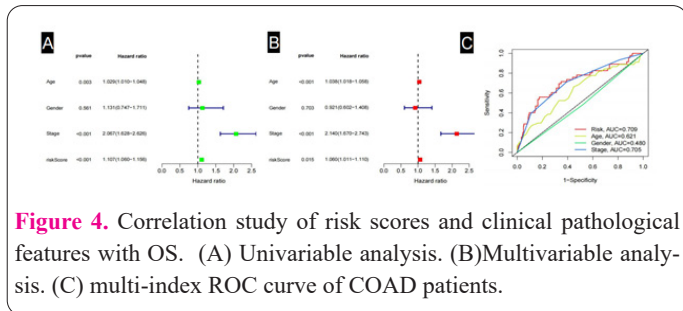


Figure 4. Correlation study of risk scores and clinical pathological features with OS. (A) Univariable analysis. (B) Multivariable analysis. (C) multi-index ROC curve of COAD patients.

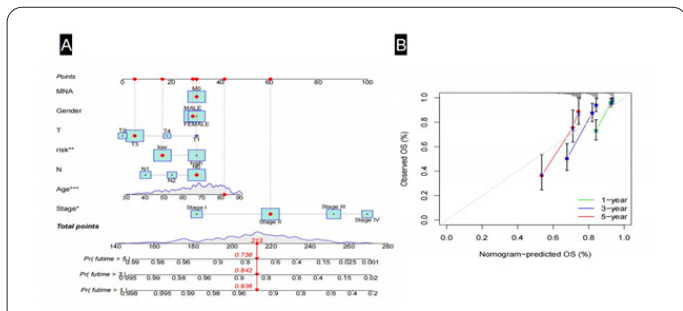


Figure 5. Development of a nomograph for forecasting OS in COAD patients. (A) Nomograph on the basis of cuprotosis-related lncRNA risk elements can predict 1-, 3-, and 5-year survivorship in COAD patients. (B) Nomograph calibration curves for predicting 1-, 3-, and 5-year survivorship.

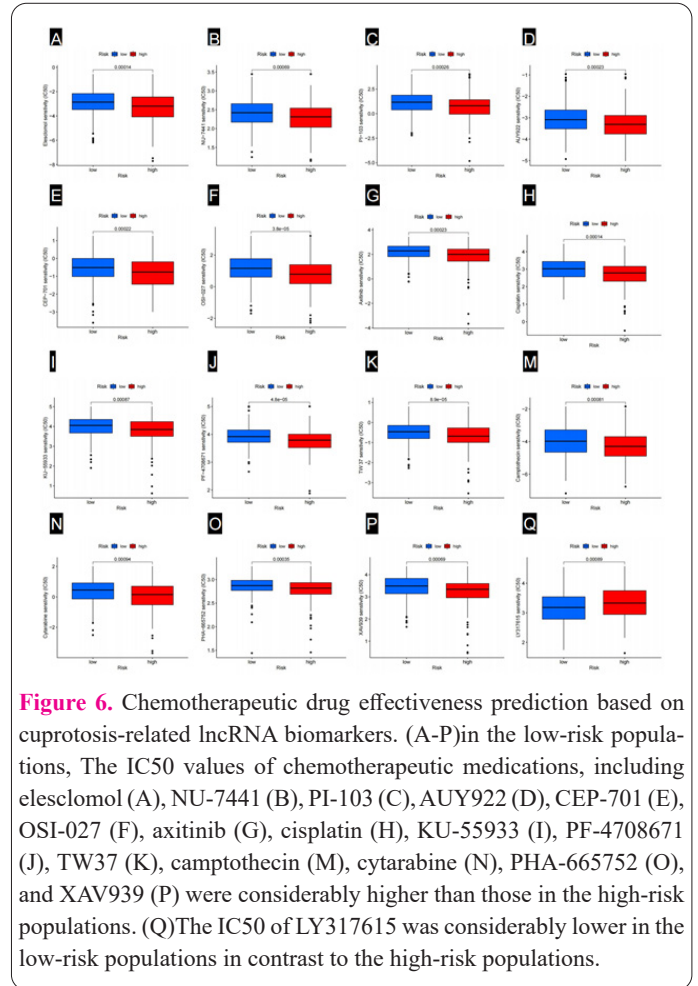


Figure 6. Chemotherapeutic drug effectiveness prediction based on cuprotosis-related lncRNA biomarkers. (A-P) in the low-risk populations, The IC50 values of chemotherapeutic medications, including elesclomol (A), NU-7441 (B), PI-103 (C), AUY922 (D), CEP-701 (E), OSI-027 (F), axitinib (G), cisplatin (H), KU-55933 (I), PF-4708671 (J), TW37 (K), camptothecin (M), cytarabine (N), PHA-665752 (O), and XAV939 (P) were considerably higher than those in the high-risk populations. (Q) The IC50 of LY317615 was considerably lower in the low-risk populations in contrast to the high-risk populations.

tothecin, cytarabine, PHA-665752, and XAV939 were dramatically lower among high-risk populations (Figures 6A-P). These chemotherapeutic drugs were more effective for high-risk populations. Conversely, the IC50 of LY317615 was dramatically lower in the low-risk populations (Figure 6Q), revealing that LY317615 was more effective in low-risk populations.

Discussion

Cuprotosis is a distinct kind of cell death caused by proteotoxic stress and mediated by copper binding to lipoylated TCA cycle enzymes (10). Studies (11, 20) have connected cuprotosis to the initiation and progression of colon and liver cancer. LncRNAs are important in biological regulation and are increasingly being recognized for their roles in prognostic prediction (21, 22). In colon cancer, many lncRNAs have been shown to be useful for predicting prognosis (23-25). However, the prognostic efficacy of cuprotosis-related lncRNA biomarkers for COAD remains unclear.

In this study, AC008494.3, SNHG7, LINC02257, ZEB1-AS1, and AC116913.1 were confirmed as cuprotosis-related lncRNAs linked to the prognosis of COAD sufferers by univariable Cox, LASSO, and multivariable Cox. Using these cuprotosis-related COAD prognosis-associated lncRNAs, five risk biomarkers were constructed. These five lncRNAs have been reported in tumors, and some of them have been reported in COAD. Wang et al. (26) reported that in a cohort of patients with COAD from TCGA, the expression level of the lncRNA AC008494.3 was positively correlated with OS, which is the same as

the findings of this study. SNHG7 expression was considerably elevated in COAD samples and lineage cells, and it was related to cancer size, lymph node metastases, distant metastases, and cancer stage. Individuals with overexpression of SNHG7 exhibited a significantly worse survivorship time than those with limited SNHG7 expression (27-29). In vitro research indicated that SNHG7 can minimize cell apoptosis and enhance COAD cell proliferation via modulating miR-193b expression and upregulating K-ras/extracellular regulated protein kinase (ERK)/cyclin D1 (30). Shan et al. (31) report that by binding to miR-216b, SNHG7 positively modulates the expressing levels of GALNT1 and vimentin, and facilitates the proliferative, metastatic, and aggressive abilities of COAD lineage cells. It's been revealed that the expressing level of SNHG7 is considerably elevated in gastric carcinoma (32), esophageal carcinoma (33), pancreatic carcinoma (34), hepatic carcinoma (35), breast cancer (36), lung carcinoma (37), cervical carcinoma (38), bladder carcinoma (39), osteosarcoma (40), prostate cancer (41), brain glioma (42), and thyroid cancer tissues and cell lines (43), suggesting it may exert an effect in the onset and developmental process of cancer.

Studies have shown that, compared to para-carcinoma tissues, the expression of LINC02257 was pronouncedly higher in COAD, bladder urothelial carcinoma, invasive breast carcinoma, bile duct carcinoma, esophageal tumor, chromophobe kidney cancer, hepatic tumor, lung cancer, rectal carcinoma, gastric tumor, thyroid tumor, and endometrioid carcinoma. The expression level of LINC02257 was related to the stage and prognoses of several malignancies, as well as the infiltration of different immunocytes. LINC02257 impacted exocellular structures and organization via the PI3K-Akt signalpath (44-47). ZEB1-AS1 was highly overexpressed in tissular samples and lineage cells derived from the hepatic tumor (48), pancreas tumor (49), gastric tumor (50), colonic and rectal tumor (51, 52), triple-negative breast tumor (53), glioma (54), and bladder tumor (55). Through miR-505/tribbles homologue 2 (TRIB2), ZEB1-AS1 boosted pancreatic tumor cell survivorship, metastasis, and aggression (49). ZEB1-AS1 promoted the developmental process of thyroid tumor via upregulating the expressing levels of lysophosphatidic acid receptor 3 and EGFR via miR-133a-3p, promoting the PI3K/AKT/mTOR pathway, enhancing the proliferation of thyroid (56). LncRNA AC116913.1 was identified as an independent prediction element in pancreatic cancer sufferers from TCGA datasets (57).

In this study, we adopted the ROC curve to estimate predictive performance (58), and the area under the ROC curve (AUC) was employed to quantify predictive ability (59).

To analyze the accurateness of the cuprotosis-related lncRNA model of risk for predicting COAD prognosis, our team separated COAD sufferers in the training set into high- and low-risk groups on the basis of the risk score mid-value of five screened lncRNA biomarkers. The survivorship analysis indicated that the high-risk sufferers had considerably worse survivorship times in contrast to the low-risk sufferers. The model of risk on the basis of five cuprotosis-related lncRNA risk biomarkers was further verified using the testing set and the entire patient population, and the results demonstrated that it had a strong prediction performance for the prognoses of COAD suf-

ferers. According to univariable and multivariable Cox analyses, the model is an independent prognostic predictor independent of clinical elements. Using five cuprotosis-related lncRNAs and clinical characteristics, we developed a nomograph to forecast OS at 1, 3, and 5 years. The nomograph calibration plots indicated that the nomograph accurately predicted the lifetime versus time curves. The anticipated patient lifetime was close to the actual patient lifetime, demonstrating that the nomograph may accurately estimate patient life expectancy. Using the pRRophetic R package, we investigated the sensitivity of two risk populations to commonly used chemotherapeutics, and our findings indicated that the model of risk was useful for predicting the efficacy of specific chemotherapeutics.

This study has certain limitations, and clinical trials are required to confirm the model of risk based on five cuprotosis-related lncRNAs. In addition, the functions of these five lncRNAs and the COAD-related mechanisms need to be further analyzed. We created a risk model based on cuprotosis-related marker lncRNAs that have been linked to the prognosis of COAD patients. The model can be used to predict OS and the effectiveness of certain chemotherapeutics, but its applicability in a larger population must be validated.

Acknowledgments

This work was supported by the Rising Star Program by Baoshan Branch, Renji Hospital, School of Medicine, Shanghai Jiao Tong University (rbxxrc-2019-008).

Conflicts of interest

The authors declare that they have no conflicts of interest.

References

1. Sung H, Ferlay J, Siegel RL, Laversanne M, Soerjomataram I, Jemal A, Bray F. Global Cancer Statistics 2020: GLOBOCAN Estimates of Incidence and Mortality Worldwide for 36 Cancers in 185 Countries. *CA Cancer J Clin* 2021; 71: 209-249.
2. Pappa KI, Polyzos A, Jacob-Hirsch J, Amariglio N, Vlachos GD, Loutradis D, Anagnostou NP. Profiling of Discrete Gynecological Cancers Reveals Novel Transcriptional Modules and Common Features Shared by Other Cancer Types and Embryonic Stem Cells. *PLoS one* 2015; 10: e0142229.
3. Dekker E, Tanis PJ, Vleugels J, Kasi PM, Wallace MB. Colorectal cancer. *Lancet* 2019; 394: 1467-1480.
4. Zhang Y, Chen Z, Li J. The current status of treatment for colorectal cancer in China: A systematic review. *Medicine (Baltimore)* 2017; 96: e8242.
5. Popescu RC, Botea F, Dumitru E, Mazilu L, Micu LG, Tocia C, Dumitru A, Croitoru A, Leopa N. Extended Lymphadenectomy for Proximal Transverse Colon Cancer: Is There a Place for Standardization?. *Medicina (Kaunas)* 2022; 58: 596.
6. Rega D, Granata V, Petrillo A, Pace U, Di Marzo M, Fusco R, D'Alessio V, Nasti G, Romano C, Avallone A. Electrochemotherapy of Primary Colon Rectum Cancer and Local Recurrence: Case Report and Prospective Analysis. *J Clin Med* 2022; 11: 2745.
7. Guo L, Wang C, Qiu X, Pu X, Chang P. Colorectal Cancer Immune Infiltrates: Significance in Patient Prognosis and Immunotherapeutic Efficacy. *Front Immunol* 2020; 11: 1052.
8. Fan XJ, Wan XB, Fu XH, Wu PH, Chen DK, Wang PN, Jiang L, Wang DH, Chen ZT, Huang Y. Phosphorylated p38, a negative prognostic biomarker, complements TNM staging prognostication in colorectal cancer. *Tumour Biol* 2014; 35: 10487-10495.

9. Puccini A, Berger MD, Zhang W, Lenz HJ. What We Know About Stage II and III Colon Cancer: It's Still Not Enough. *Target Oncol* 2017; 12: 265-275.
10. Tsvetkov P, Coy S, Petrova B, Dreishpoon M, Verma A, Abdusamad M, Rossen J, Joesch-Cohen L, Humeidi R, Spangler RD. Copper induces cell death by targeting lipoylated TCA cycle proteins. *Science* 2022; 375: 1254-1261.
11. Aubert L, Nandagopal N, Steinhart Z, Lavoie G, Nourreddine S, Berman J, Saba-El-Leil MK, Papadopoli D, Lin S, Hart T. Copper bioavailability is a KRAS-specific vulnerability in colorectal cancer. *Nat Commun* 2020; 11: 3701.
12. Bridges MC, Daulagala AC, Kourtidis A. LNCcation: lncRNA localization and function. *J Cell Biol* 2021; 220: e202009045.
13. Taniue K, Akimitsu N. The Functions and Unique Features of LncRNAs in Cancer Development and Tumorigenesis. *Int J Mol Sci* 2021; 22: 632.
14. Chen S, Shen X. Long noncoding RNAs: functions and mechanisms in colon cancer. *Mol Cancer* 2020; 19: 167.
15. Tan YT, Lin JF, Li T, Li JJ, Xu RH, Ju HQ. LncRNA-mediated posttranslational modifications and reprogramming of energy metabolism in cancer. *Cancer Commun (Lond)* 2021; 41: 109-120.
16. Lin W, Zhou Q, Wang CQ, Zhu L, Bi C, Zhang S, Wang X, Jin H. LncRNAs regulate metabolism in cancer. *Int J Biol Sci* 2020; 16: 1194-1206.
17. Polishchuk EV, Merolla A, Lichtmanegger J, Romano A, Indrieri A, Ilyechova EY, Concilli M, De Cegli R, Crispino R, Mariniello M. Activation of Autophagy, Observed in Liver Tissues from Patients with Wilson Disease and From ATP7B-Deficient Animals, Protects Hepatocytes from Copper-Induced Apoptosis. *Gastroenterology* 2019; 156: 1173-1189.
18. Kahlson MA, Dixon SJ. Copper-induced cell death. *Science* 2022; 375: 1231-1232.
19. Dong J, Wang X, Xu C, Gao M, Wang S, Zhang J, Tong H, Wang L, Han Y, Cheng N. Inhibiting NLRP3 inflammasome activation prevents copper-induced neuropathology in a murine model of Wilson's disease. *Cell Death Dis* 2021; 12: 87.
20. Ren X, Li Y, Zhou Y, Hu W, Yang C, Jing Q, Zhou C, Wang X, Hu J, Wang L. Overcoming the compensatory elevation of NRF2 renders hepatocellular carcinoma cells more vulnerable to disulfiram/copper-induced ferroptosis. *Redox Biol* 2021; 46: 102122.
21. Statello L, Guo CJ, Chen LL, Huarte M. Gene regulation by long non-coding RNAs and its biological functions. *Nat Rev Mol Cell Biol* 2021; 22: 96-118.
22. Wang W, Lou W, Ding B, Yang B, Lu H, Kong Q, Fan W. A novel mRNA-miRNA-lncRNA competing endogenous RNA triple subnetwork associated with prognosis of pancreatic cancer. *Aging* 2019; 11: 2610-2627.
23. Cheng L, Han T, Zhang Z, Yi P, Zhang C, Zhang S, Peng W. Identification and Validation of Six Autophagy-related Long Non-coding RNAs as Prognostic Signature in Colorectal Cancer. *Int J Med Sci* 2021; 18: 88-98.
24. Zhou W, Zhang S, Li HB, Cai Z, Tang S, Chen LX, Lang JY, Chen Z, Chen XL. Development of Prognostic Indicator Based on Autophagy-Related lncRNA Analysis in Colon Adenocarcinoma. *Biomed Res Int* 2020; 9807918.
25. Dastmalchi N, Safaralizadeh R, Nargesi MM. LncRNAs: Potential Novel Prognostic and Diagnostic Biomarkers in Colorectal Cancer. *Curr Med Chem* 2020; 27: 5067-5077.
26. Wang Y, Liu J, Ren F, Chu Y, Cui B. Identification and Validation of a Four-Long Non-coding RNA Signature Associated with Immune Infiltration and Prognosis in Colon Cancer. *Front Genet* 2021; 12: 671128.
27. Hu Y, Wang L, Li Z, Wan Z, Shao M, Wu S, Wang G. Potential Prognostic and Diagnostic Values of CDC6, CDC45, ORC6 and SNHG7 in Colorectal Cancer. *Onco Targets Ther* 2019; 12: 11609-11621.
28. Ziaee F, Hajjari M, Kazeminezhad RS, Behmanesh M. SNHG7 and FAIM2 are up-regulated and co-expressed in colorectal adenocarcinoma tissues. *Klin Onkol* 2020; 33: 445-449.
29. Li Y, Zeng C, Hu J, Pan Y, Shan Y, Liu B, Jia L. Long non-coding RNA-SNHG7 acts as a target of miR-34a to increase GALNT7 level and regulate PI3K/Akt/mTOR pathway in colorectal cancer progression. *J Hematol Oncol* 2018; 11: 89.
30. Liu KL, Wu J, Li WK, Li NS, Li Q, Lao YQ. LncRNA SNHG7 is an Oncogenic Biomarker Interacting with MicroRNA-193b in Colon Carcinogenesis. *Clin Lab* 2019; 65 190501.
31. Shan Y, Ma J, Pan Y, Hu J, Liu B, Jia L. LncRNA SNHG7 sponges miR-216b to promote proliferation and liver metastasis of colorectal cancer through upregulating GALNT1. *Cell Death Dis* 2018; 9: 722.
32. Zhao Z, Liu X. LncRNA SNHG7 Regulates Gastric Cancer Progression by miR-485-5p. *J Oncol* 2021; 6147962.
33. Xu LJ, Yu XJ, Wei B, Hui HX, Sun Y, Dai J, Chen XF. LncRNA SNHG7 promotes the proliferation of esophageal cancer cells and inhibits its apoptosis. *Eur Rev Med Pharmacol Sci* 2018; 22: 2653-2661.
34. Cheng D, Fan J, Ma Y, Zhou Y, Qin K, Shi M, Yang J. LncRNA SNHG7 promotes pancreatic cancer proliferation through ID4 by sponging miR-342-3p. *Cell Biosci* 2019; 9: 28.
35. Cui H, Zhang Y, Zhang Q, Chen W, Zhao H, Liang J. A comprehensive genome-wide analysis of long noncoding RNA expression profile in hepatocellular carcinoma. *Cancer Med* 2017; 6: 2932-2941.
36. Li Y, Guo X, Wei Y. LncRNA SNHG7 inhibits proliferation and invasion of breast cancer cells by regulating miR-15a expression. *J BUON* 2020; 25: 1792-1798.
37. Li L, Ye D, Liu L, Li X, Liu J, Su S, Lu W, Yu Z. Long Noncoding RNA SNHG7 Accelerates Proliferation, Migration and Invasion of Non-Small Cell Lung Cancer Cells by Suppressing miR-181a-5p Through AKT/mTOR Signaling Pathway. *Cancer Manag Res* 2020; 12: 8303-8312.
38. Zeng J, Ma YX, Liu ZH, Zeng YL. LncRNA SNHG7 contributes to cell proliferation, invasion and prognosis of cervical cancer. *Eur Rev Med Pharmacol Sci* 2019; 23: 9277-9285.
39. Chen Y, Peng Y, Xu Z, Ge B, Xiang X, Zhang T, Gao L, Shi H, Wang C, Huang J. Knockdown of lncRNA SNHG7 inhibited cell proliferation and migration in bladder cancer through activating Wnt/ β -catenin pathway. *Pathol Res Pract* 2019; 215: 302-307.
40. Deng Y, Zhao F, Zhang Z, Sun F, Wang M. Long Noncoding RNA SNHG7 Promotes the Tumor Growth and Epithelial-to-Mesenchymal Transition via Regulation of miR-34a Signals in Osteosarcoma. *Cancer Biother Radiopharm* 2018; 33: 365-372.
41. Han Y, Hu H, Zhou J. Knockdown of LncRNA SNHG7 inhibited epithelial-mesenchymal transition in prostate cancer through miR-324-3p/WNT2B axis in vitro. *Pathol Res Pract* 2019; 215: 152537.
42. Ren J, Yang Y, Xue J, Xi Z, Hu L, Pan SJ, Sun Q. Long noncoding RNA SNHG7 promotes the progression and growth of glioblastoma via inhibition of miR-5095. *Biochem Biophys Res Commun* 2018; 496: 712-718.
43. Wang YH, Huo BL, Li C, Ma G, Cao W. Knockdown of long noncoding RNA SNHG7 inhibits the proliferation and promotes apoptosis of thyroid cancer cells by downregulating BDNF. *Eur Rev Med Pharmacol Sci* 2019; 23: 4815-4821.
44. Xiao J, Liu Y, Yi J, Liu X. LINC02257, an Enhancer RNA of Prognostic Value in Colon Adenocarcinoma, Correlates with Multi-Omics Immunotherapy-Related Analysis in 33 Cancers. *Front Mol Biosci* 2021; 8: 646786.

45. Huang X, Cai W, Yuan W, Peng S. Identification of key lncRNAs as prognostic prediction models for colorectal cancer based on LASSO. *Int J Clin Exp Pathol* 2020; 13: 675-684.
46. Wang X, Zhou J, Xu M, Yan Y, Huang L, Kuang Y, Liu Y, Li P, Zheng W, Liu H. A 15-lncRNA signature predicts survival and functions as a ceRNA in patients with colorectal cancer. *Cancer Manag Res* 2018; 10: 5799-5806.
47. Lin G, Wang H, Wu Y, Wang K, Li G. Hub Long Noncoding RNAs with m6A Modification for Signatures and Prognostic Values in Kidney Renal Clear Cell Carcinoma. *Front Mol Biosci* 2021; 8: 682471.
48. Mu B, Lv C, Liu Q, Yang H. Long non-coding RNA ZEB1-AS1 promotes proliferation and metastasis of hepatocellular carcinoma cells by targeting miR-299-3p/E2F1 axis. *J Biochem* 2021; 170 (1): 41-50.
49. Wei G, Lu T, Shen J, Wang J. LncRNA ZEB1-AS1 promotes pancreatic cancer progression by regulating miR-505-3p/TRIB2 axis. *Biochem Biophys Res Commun* 2020; 528: 644-649.
50. Ma MH, An JX, Zhang C, Liu J, Liang Y, Zhang CD, Zhang Z, Dai DQ. ZEB1-AS1 initiates a miRNA-mediated ceRNA network to facilitate gastric cancer progression. *Cancer Cell Int* 2019; 19: 27.
51. Wu G, Xue M, Zhao Y, Han Y, Li C, Zhang S, Zhang J, Xu, J. Long noncoding RNA ZEB1-AS1 acts as a Sponge of miR-141-3p to Inhibit Cell Proliferation in Colorectal Cancer. *Int J Med Sci* 2020; 17: 1589-1597.
52. Fu J, Cui Y. Long noncoding RNA ZEB1-AS1 expression predicts progression and poor prognosis of colorectal cancer. *Int J Biol Markers* 2017; 32: e428–e433.
53. Luo N, Zhang K, Li X, Hu Y. ZEB1 induced-upregulation of long noncoding RNA ZEB1-AS1 facilitates the progression of triple negative breast cancer by binding with ELAVL1 to maintain the stability of ZEB1 mRNA. *J Cell Biochem* 2020; 121: 4176-4187.
54. Wei N, Wei H, Zhang H. Long non-coding RNA ZEB1-AS1 promotes glioma cell proliferation, migration and invasion through regulating miR-577. *Eur Rev Med Pharmacol Sci* 2018; 22: 3085-3093.
55. Zhao X, Wang D, Ding Y, Zhou J, Liu G, Ji Z. LncRNA ZEB1-AS1 promotes migration and metastasis of bladder cancer cells by post-transcriptional activation of ZEB1. *Int J Mol Med* 2019; 44: 196-206.
56. Xia W, Jie W. ZEB1-AS1/miR-133a-3p/LPAR3/EGFR axis promotes the progression of thyroid cancer by regulating PI3K/AKT/mTOR pathway. *Cancer Cell Int* 2020; 20: 94.
57. Wei C, Liang Q, Li X, Li H, Liu Y, Huang X, Chen X, Guo Y, Li J. Bioinformatics profiling utilized a nine immune-related long noncoding RNA signature as a prognostic target for pancreatic cancer. *J Cell Biochem* 2019; 120: 14916-14927.
58. Kamarudin AN, Cox T, Kolamunnage-Dona R. Time-dependent ROC curve analysis in medical research: current methods and applications. *BMC Med Res Methodol* 2017; 17: 53.
59. Wolbers M, Koller MT, Witteman JC, Steyerberg, E. W. Prognostic models with competing risks: methods and application to coronary risk prediction. *Epidemiology* 2009; 20: 555-561.